原始銀河の進化と Lyman α Emitters

森正夫

筑波大学計算科学研究センター
(2008年4月1日付けで専修大学から異動しました)

Lyα emitters and Lyα blobs

Matsuda et al., AJ, 128, [redacted] (2004)

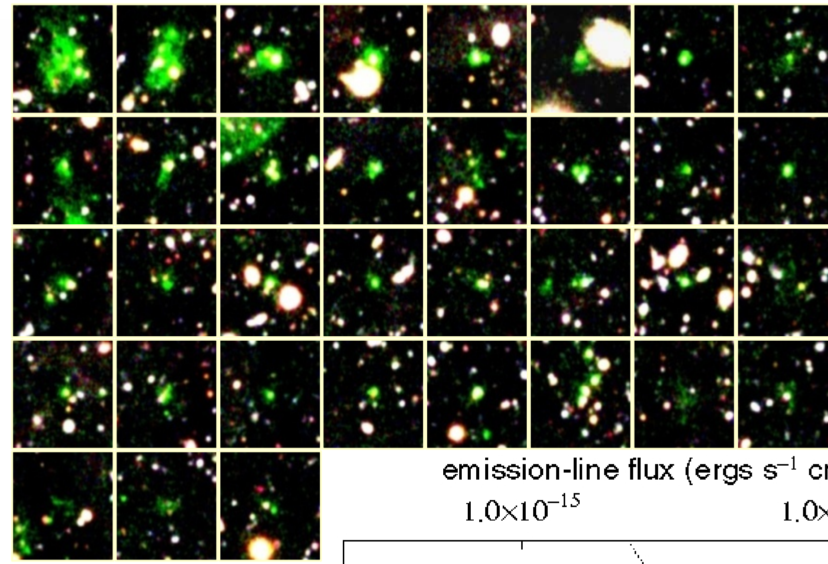

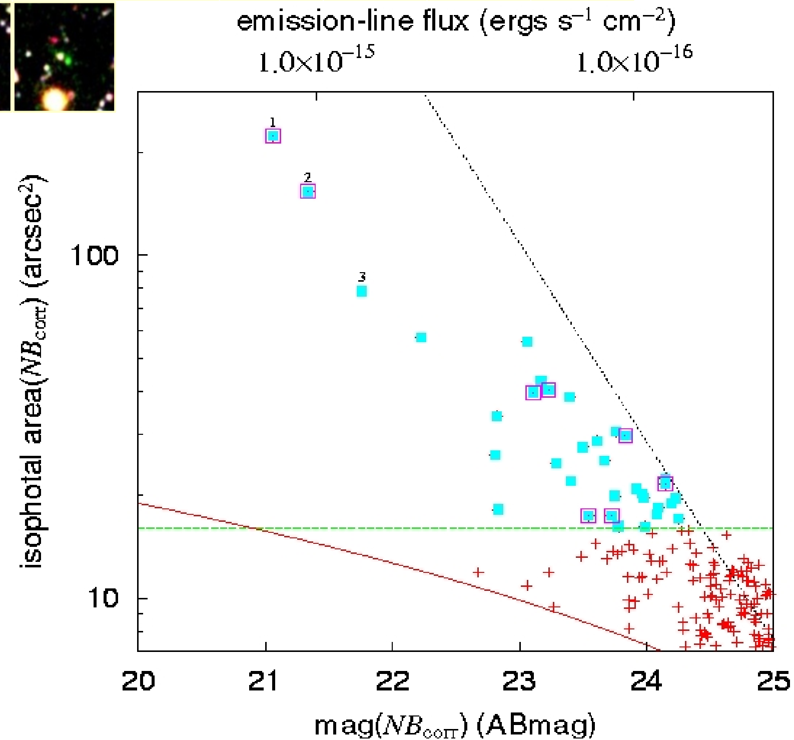

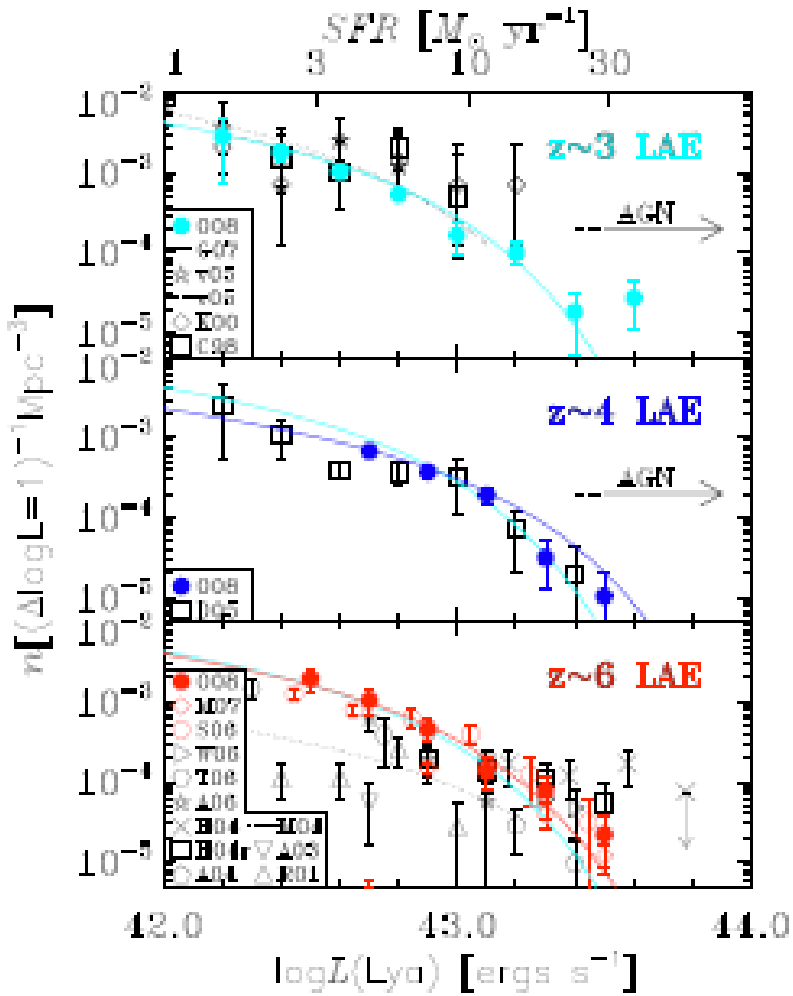

Ouchi. et al. ApJS, 176, 3010 (2008)

Mass of Lyman alpha emitters

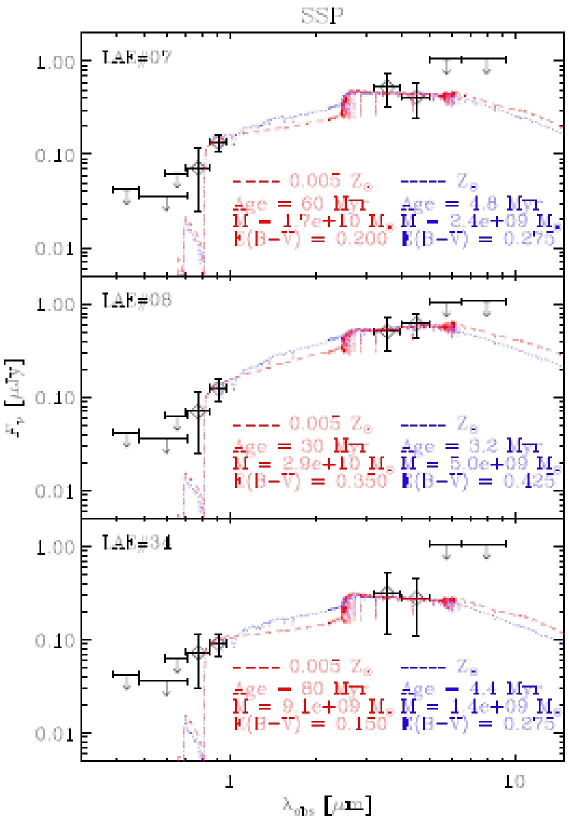

FIG. 3.— Best fit SSP models to the three IRAC-detected $z \sim 5.7$ LAEs. The blue-dotted (red-dashed) line is for a model with $Z = Z_\odot$ ($0.005\ Z_\odot$). The observed SEDs are plotted as diamonds with error bars. The horizontal error bars indicate approximately the FWHM of the passbands. When an object is undetected in a certain passband, the corresponding 3σ upper limit is shown. Note that a 30% fractional error is added to the i'-band to account for the Lyα line contribution.

TABLE 2
BEST-FIT MODEL PARAMETERS

	Age [Myr]	Mass [$M_\odot$]	$E(B-V)$	χ^2_ν	Age [Myr]	Mass [$M_\odot$]	$E(B-V)$	χ^2_ν
		SSP, $Z_\odot$				SSP, 0.005 $Z_\odot$		
LAE#07	4.8	2.4×10^9	0.275	2.05	60	1.7×10^{10}	0.200	1.97
LAE#08	3.2	5.0×10^9	0.425	2.19	30	2.9×10^{10}	0.350	2.20
LAE#34	4.4	1.4×10^9	0.275	2.42	80	9.1×10^9	0.150	2.36
		Constant SFR, $Z_\odot$				Constant SFR, 0.005 $Z_\odot$		
LAE#07	5.0	4.5×10^9	0.375	2.14	720	2.6×10^{10}	0.175	2.19
LAE#08	4.8	6.9×10^9	0.425	2.19	720	3.9×10^{10}	0.225	2.18
LAE#34	720	1.1×10^{10}	0.100	2.47	900	1.7×10^{10}	0.150	2.37
		SSP, $Z_\odot$, No Extinction				SSP, 0.005 $Z_\odot$, No Extinction		
LAE#07	90	9.0×10^9	0.000	1.25	260	1.7×10^{10}	0.000	1.05
LAE#08	130	1.4×10^{10}	0.000	1.45	320	2.3×10^{10}	0.000	1.28
LAE#34	80	5.1×10^9	0.000	1.41	230	9.2×10^9	0.000	1.27

Lai et al., ApJ, 635, 704 (2007)

Low mass populations

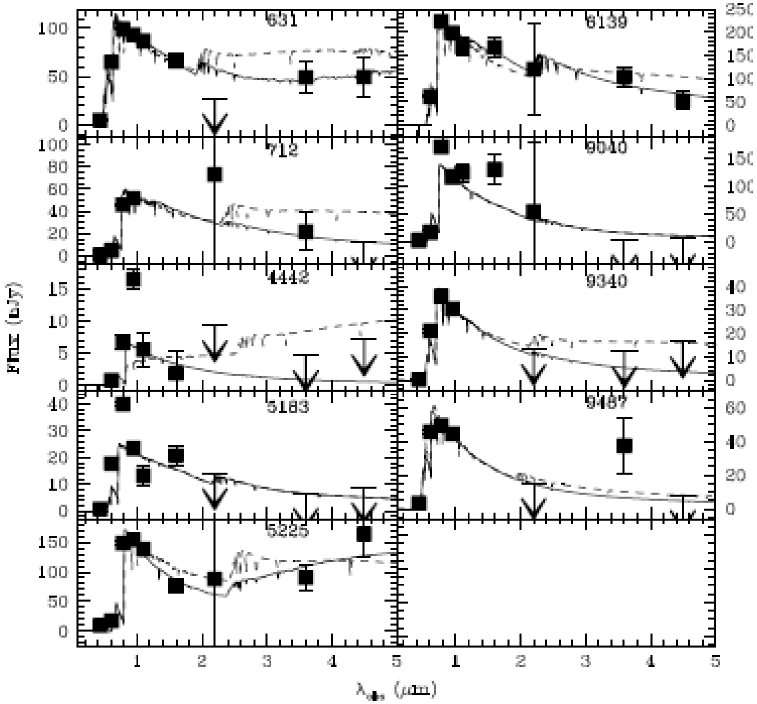

Fig. 5.— Plots of the best double instantaneous burst model (2BP) fits (solid lines) to the observations (squares) and our 1 σ upper limit estimates (arrows). The best, most massive acceptable 2BP models are also shown (dashed lines). The masses, ages, extinctions of each of these models are listed in Table 5.

Table 5. Best Double Instantaneous Burst SFH (2BP) Fits to the Observations

UID	Age 10^6 yr	Mass $10^8 M_\odot$	2nd Burst Age (10^6 yr)	2nd Burst Mass (%)	A_V	$P(\chi^2_{\nu} > \chi^2_{\nu_0})$	Age_{max} 10^6 yr	$Mass_{max}$ $10^8 M_\odot$
631	8.5	1.56	8	50	0.15	73.42	1209.0	30.9
712	16.	0.68	3.0	50	0.2	94.31	1010.	22.7
4442	2.0	0.065	1	1	0	96.82	870.0	11.4
5183^a	17.	1.09	13.	1	0.2	3.28	17.	1.06
5225	4.5	1.28	0.5	2	0.0	56.42	1000.	73.8
6139	20.	8.70	4.5	10	0.2	81.28	1006.	50.38
9040^a	7.0	1.36	2.5	1	0.0	0.04	7.0	1.36
9340	1.5	0.18	1.0	99	0.0	100.00	1200.	7.47
9487	1.0	0.61	0.5	8	0.15	6.30	1200.	1.85

$10^8 M_\odot$

Note. — Listed are the age, total mass, and extinction of the object, as well as the age of the second burst and the fraction of the total stellar mass it contains, that resulted in the lowest values of χ^2_{ν}.

^a Object failed to be properly fitted at the 95% confidence level

Pirzkal et al. ApJ, 667, 49 (2007)

Mass of Lyman alpha blobs

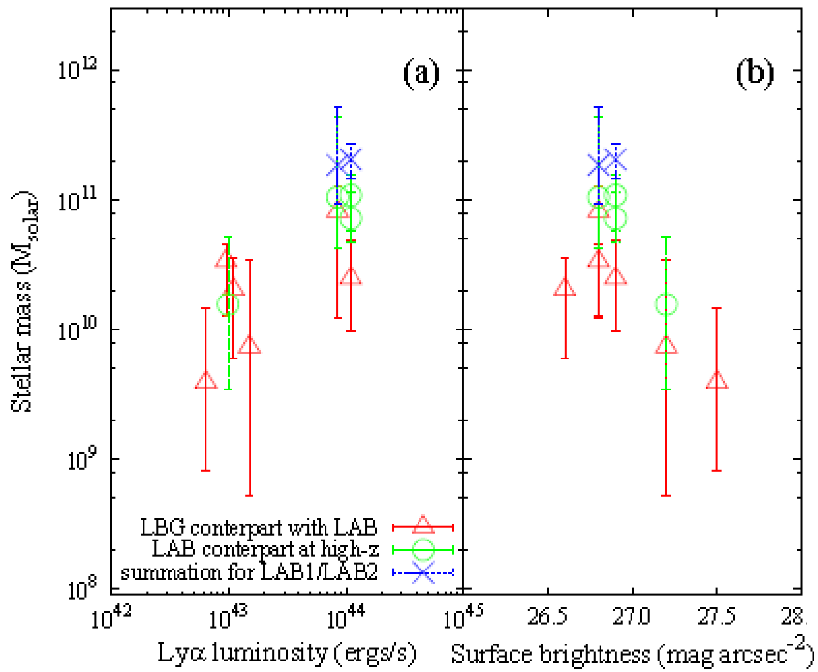

Fig. 3. (a) Lyα luminosity vs. the stellar mass of the NIR-counterpart candidates. (b) Surface brightness of Lyα vs. the stellar mass of the NIR-counterpart candidates (see text). The redshift of NIR objects is assumed to be $z = 0.1$. LBG counterparts associated with LABs are indicated with open triangles (red) and K-selected objects expected to be associated with LAB, but with no LBGs, are indicated with open circles (green). Since LAB1 and LAB2 include several NIR counterparts, the total stellar masses in each LAB are indicated with blue crosses.

$10^{10}M_{\odot}$

Table 3. The photometric redshift and stellar mass of NIR counterparts

LAB	Object ID *	z_{spec} †	z_{photo}	Age ‡ (Gyr)	E(B-V) ‡ (mag)	Mv ‡ (mag)	Stellar Mass ‡ ($10^{10} M_{\odot}$)
LAB1	C11	3.109	2.83	1.80	0.08	-22.32	$2.5^{+2.4}_{-1.5}$
	#3	-	2.85	1.80	0.20	-22.59	$7.2^{+4.3}_{-2.5}$
	#4	-	2.61	1.61	0.18	-23.19	$10.9^{+4.8}_{-5.0}$
LAB2	M14 §	3.091	3.19	1.80	0.22	-22.64	$8.1^{+4.8}_{-6.9}$
	#4	-	2.61	0.20	0.40	-23.05	$10.5^{+32.6}_{-6.3}$
LAB7	M4	3.093	2.70	0.57	0.06	-21.75	$0.7^{+2.6}_{-0.7}$
LAB16	-	-	2.70	0.06	0.20	-22.50	$1.6^{+3.5}_{-1.2}$
LAB20	C12	3.118	2.85	0.57	0.00	-21.43	$0.4^{+1.1}_{-0.3}$
LAB30	D3	3.086	3.31	1.61	0.08	-22.74	$3.4^{+1.1}_{-2.1}$
LAB31	C4	3.076	3.19	1.80	0.00	-22.04	$2.0^{+1.5}_{-1.4}$

* ID of LBGs is referred from Steidel et al. (2003a).
† The redshifts of LBGs are referred from Steidel et al. (2003a).
‡ The redshifts are assumed to be $z = 0.1$ when the SEDs are calculated.
§ The associated NIR object of M14 is located at 0''9 apart from the peak of the rest-frame UV sour

Uchimoto et al., PASJ, 60, 638 (2008)

Characteristics

	Lya emitters	Lya blobs
Lya luminosity:	10^{42-43}	10^{42-44} erg/s
Size (Lya):	a few kpc	10-100 kpc
Morphology:		
Lya:	extended	very extended
UV:	compact	scattered
Stellar mass:	$10^{8-10}\ M_\odot$	$\sim 10^{10-11}\ M_\odot$
SFR:	~ 1-$\sim 10\ M_\odot\ yr^{-1}$	~ 10-$100\ M_\odot\ yr^{-1}$

Possible models of Lya emission

- Recombination
- Cooling radiation
  - Gravitationally heated gas in pre-galactic halo
  - Shock heating by supernova driven galactic wind

Galaxy formation and supernovae

- 銀河全体の重力ポテンシャルエネルギー：　Eg = E(M)
  ※NFW プロファイルを仮定
- 銀河内の全超新星によって発生する熱エネルギー：
  Et = E(M)
  ※全質量の1%が短時間で星になったとした場合

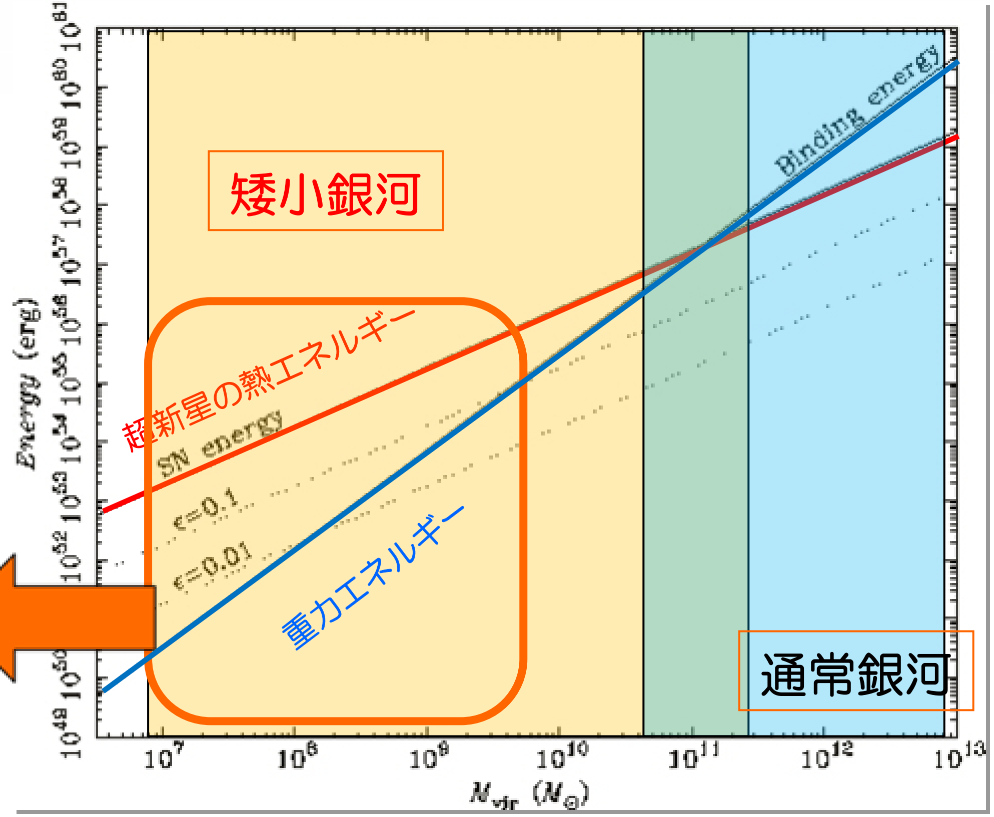

銀河の総質量 M

- ➢ 超新星の熱エネルギーが卓越
- ➢ 圧力勾配によりガスの流出
- ➢ 銀河風の発生
- ➢ 大質量のガスの放出
- ➢ 星形成の抑止
- ➢ 銀河形成が終わる

→ Negative Effect: 輻射輸送による熱エネルギーの散逸？
Positive Effect: 超新星によって放出されたガスから星形成？

→ **現実的な数値シミュレーション**

3D hydrodynamics model

We consider a forming galaxy undergoing multitudinous supernova explosions as a possible model of Lyman α emitters.

To verify this model, a high-resolution hydrodynamic simulation is performed using 1024^3 grid points, where supernova remnants are resolved with sufficient accuracy.

Numerical simulation:

- Three-dimensional hydrodynamics
- Gravity of dark matter halos (fixed potential)
- Radiative cooling (including H_2 molecule and metals)
- Star formation
- Supernova feedback (thermal energy and metals)

Spectral Energy Distribution

Emission from stars

Population synthesis model: Fioc 1997 (PÉGASE)

Emission from gas

Collisional ionization equilibrium: Sutherland & Dopita 1993
(MAPPING III)

- **Bound-bound emission**
- **Free-bound emission**
- **Free-free emission**
- **Two-photon emission**

Dust extinction

$$E(B-V)=(N/9.2\times10^{21}\ \mathrm{cm}^{-2})\times10^{[Fe/H]}$$

Extinction curve: $\langle A_{\lambda}/A_{B}\rangle$ **Pei 1992**

$M = 10^8\ M_\odot$

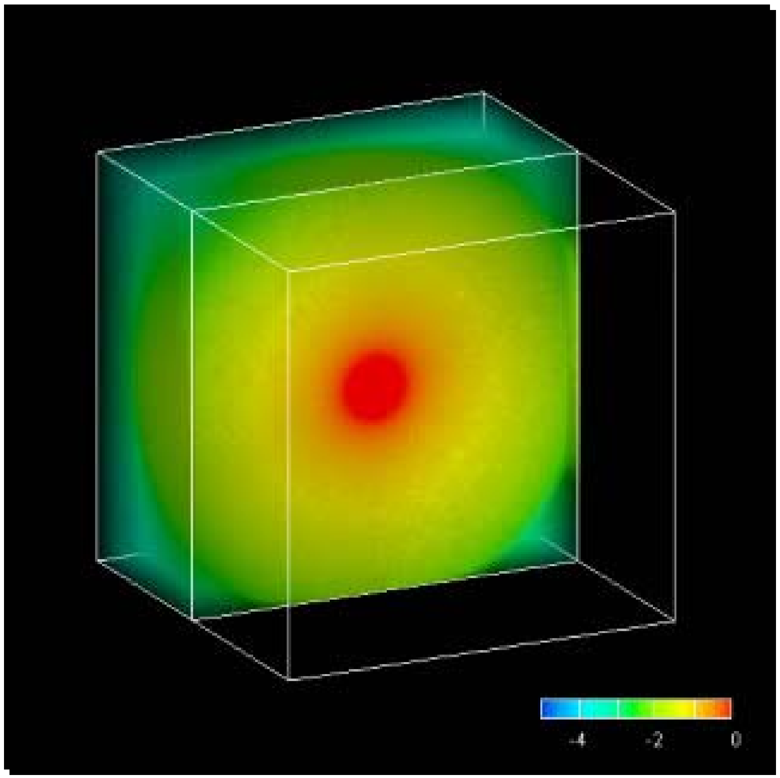

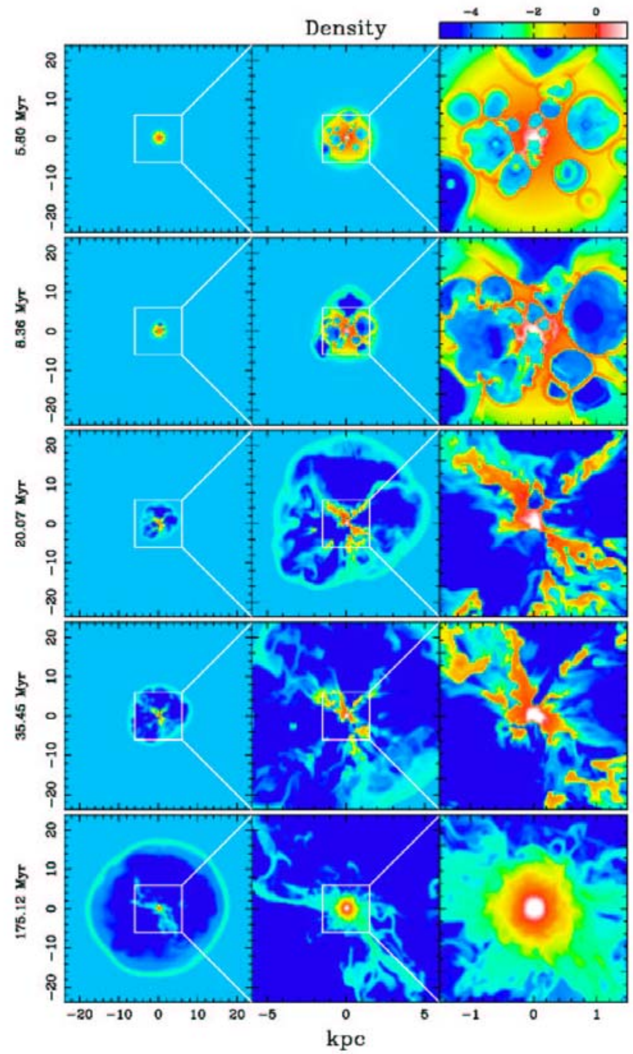

Mori, Ferrara & Madau, ApJ, 571, 49 (2002)

$M=10^{11}M_{\odot}$

Total Mass: $10^{11}\ M_{\odot}$
Gas Mass: $1.3\times10^{10}\ M_{\odot}$
No. of Subunits: 20
Box Size: 134 kpc
Grid Points: 1024^3

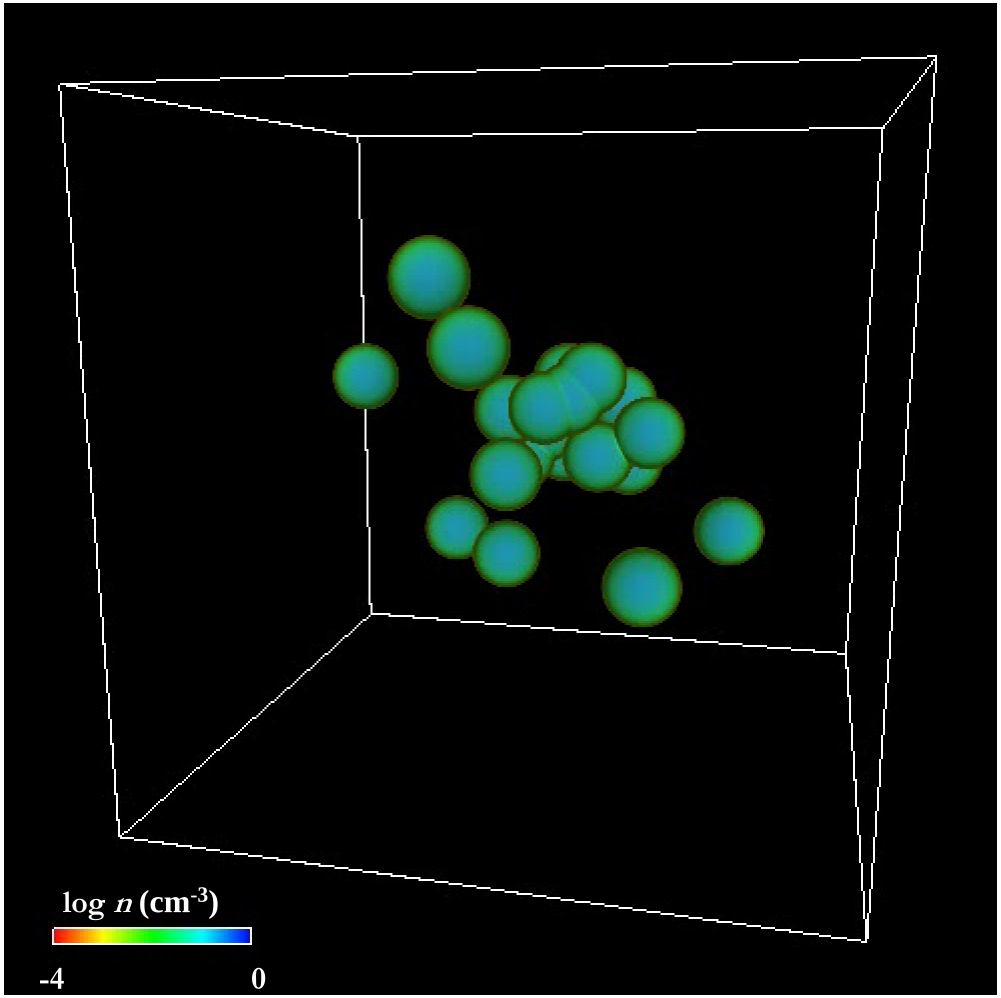

Mori & Umemura, Nature, 440, 640 (2006)

SED : Gas and Stars

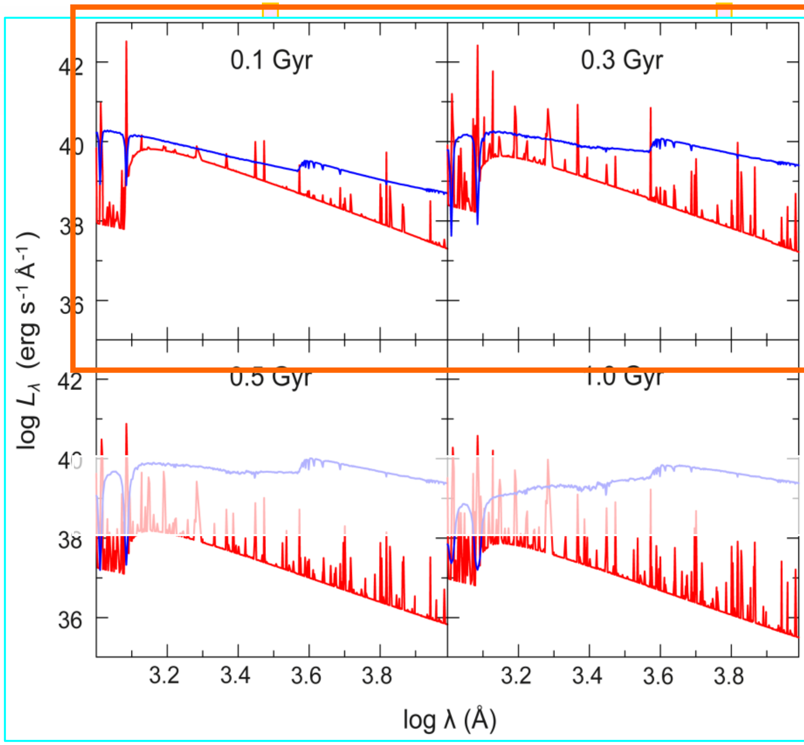

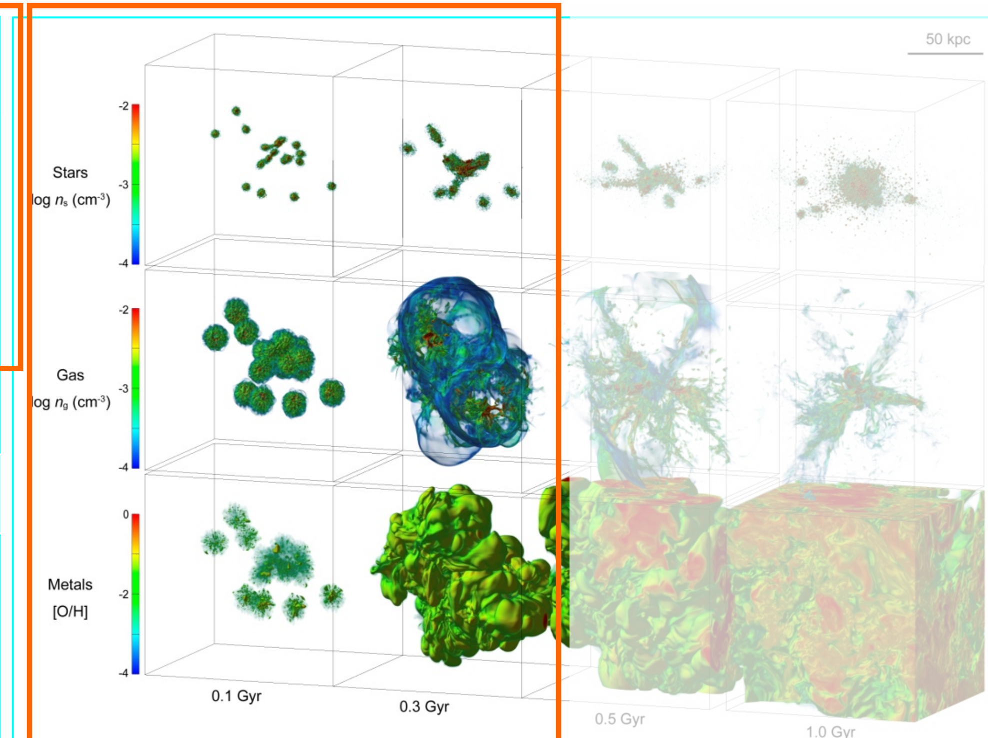

The red (blue) lines indicate the emission from gas (stellar) component.
The absolute luminosities of Lyman α line emission are 2.0×10^{43} erg s^{-1}, 1.6×10^{43} erg s^{-1}, 4.6×10^{41} erg s^{-1}, and 2.3×10^{41} erg s^{-1} at the elapsed time of 0.1 Gyr, 0.3 Gyr, 0.5 Gyr, and 1 Gyr
In the first 0.3 Gyr, the luminosities completely match the observed Ly α luminosities of Ly α emitters.

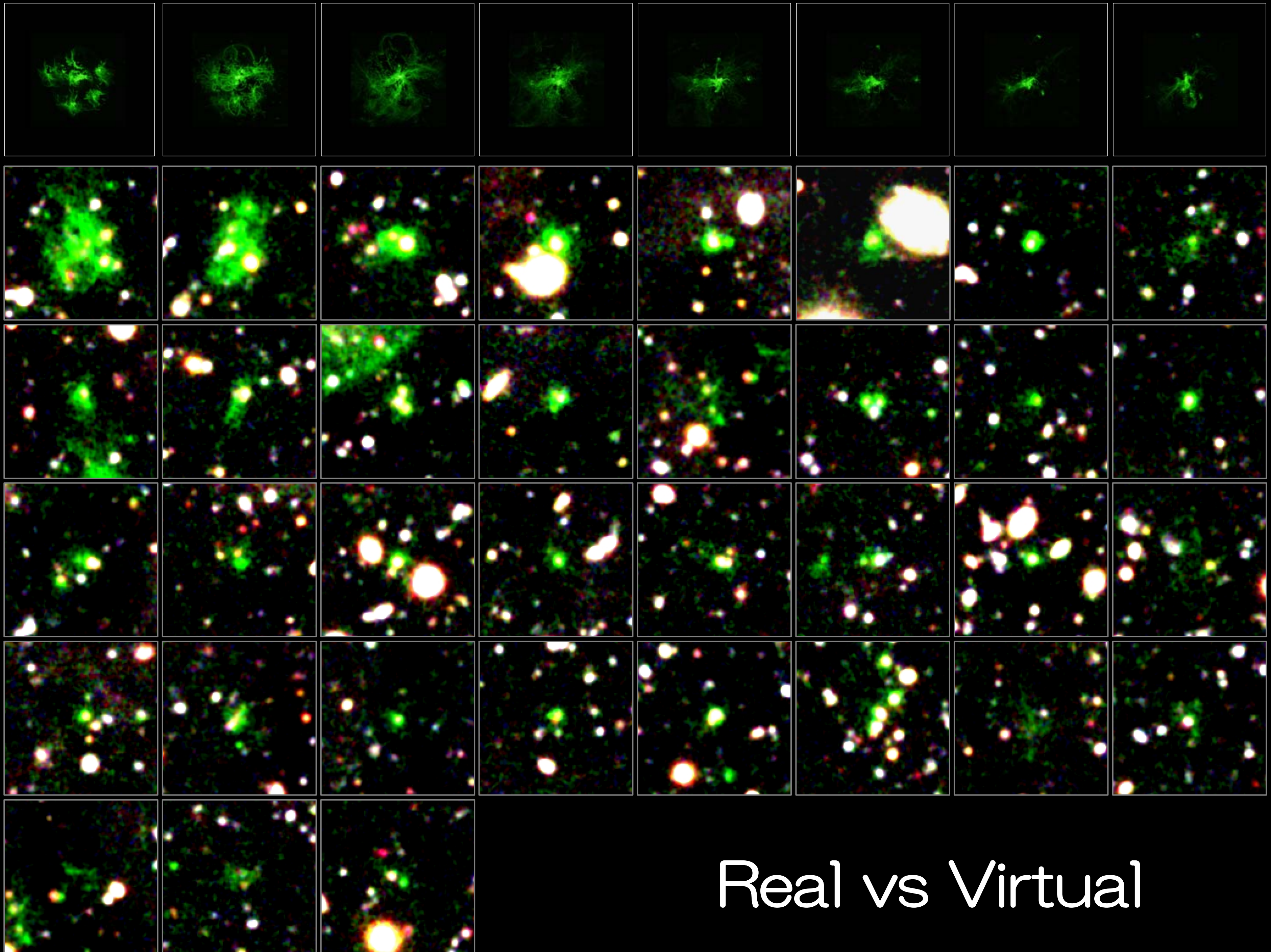

Real vs Virtual

SED : Gas and Stars

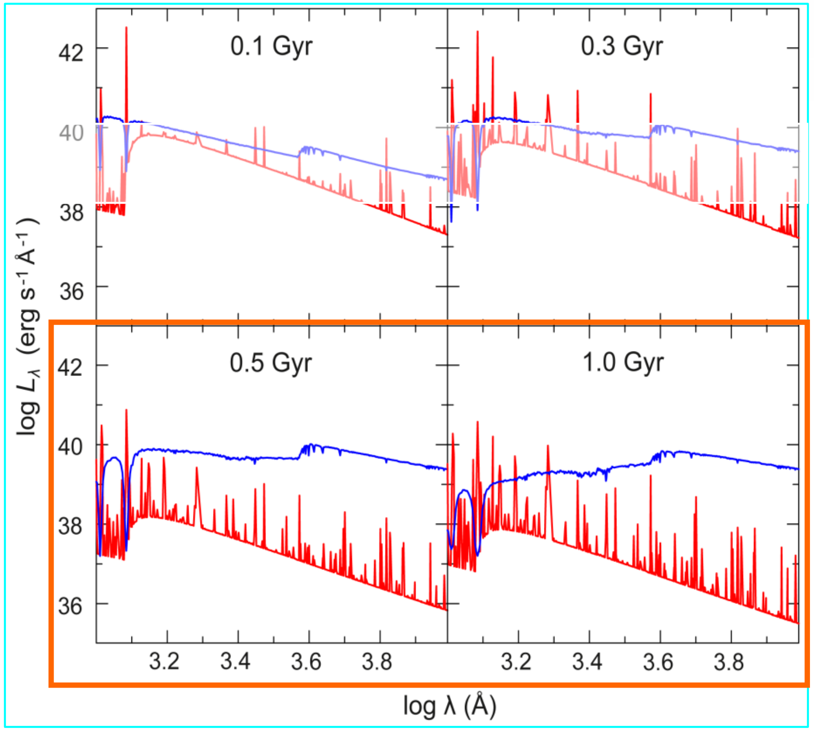

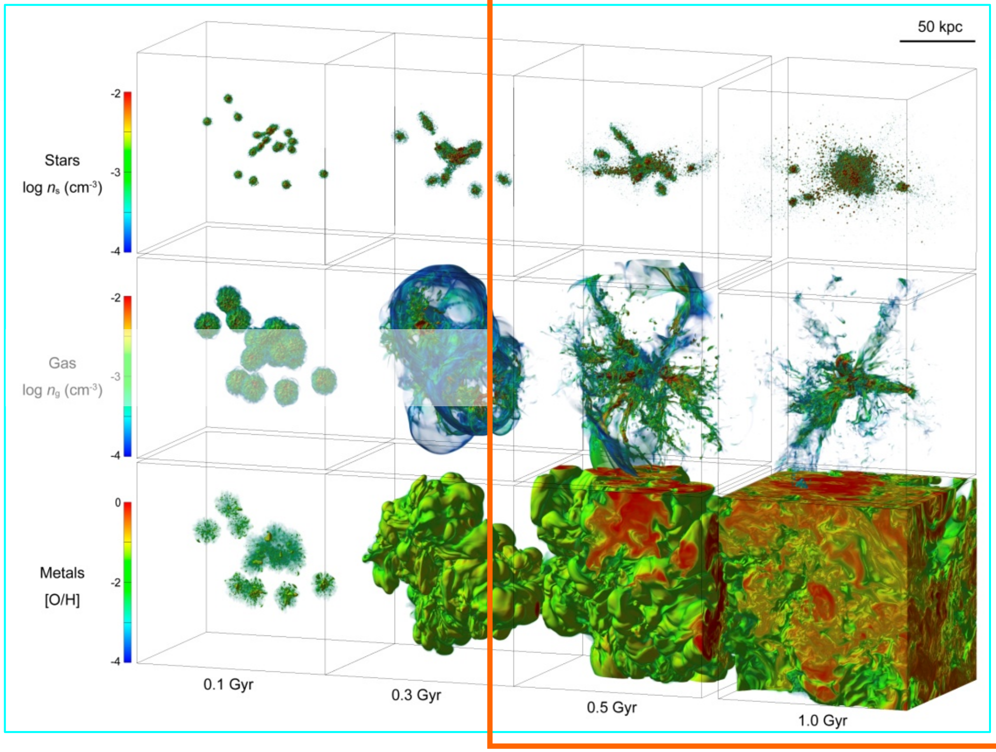

After 300 Myr, the Lyα luminosity declines to less than the observed level. Then, the SED becomes dominated by stellar continuum emission.

The galaxy in this phase is featured with diffuse, asymmetric structures, and outflows of 100~500 km s^{-1}.

The total stellar mass is 9.3×10^9 $M_\odot$, and the mass of 1.5×10^9 $M_\odot$ is involved in the outflows at z=3.

The X-ray luminosity changes from 10^{42} erg s^{-1} at 300 Myr to ~10^{41} erg s^{-1} around 1 Gyr.

These features look quite similar to those observed for Lyman Break Galaxies.

Evolution of Ly α emission and stellar continuum emission

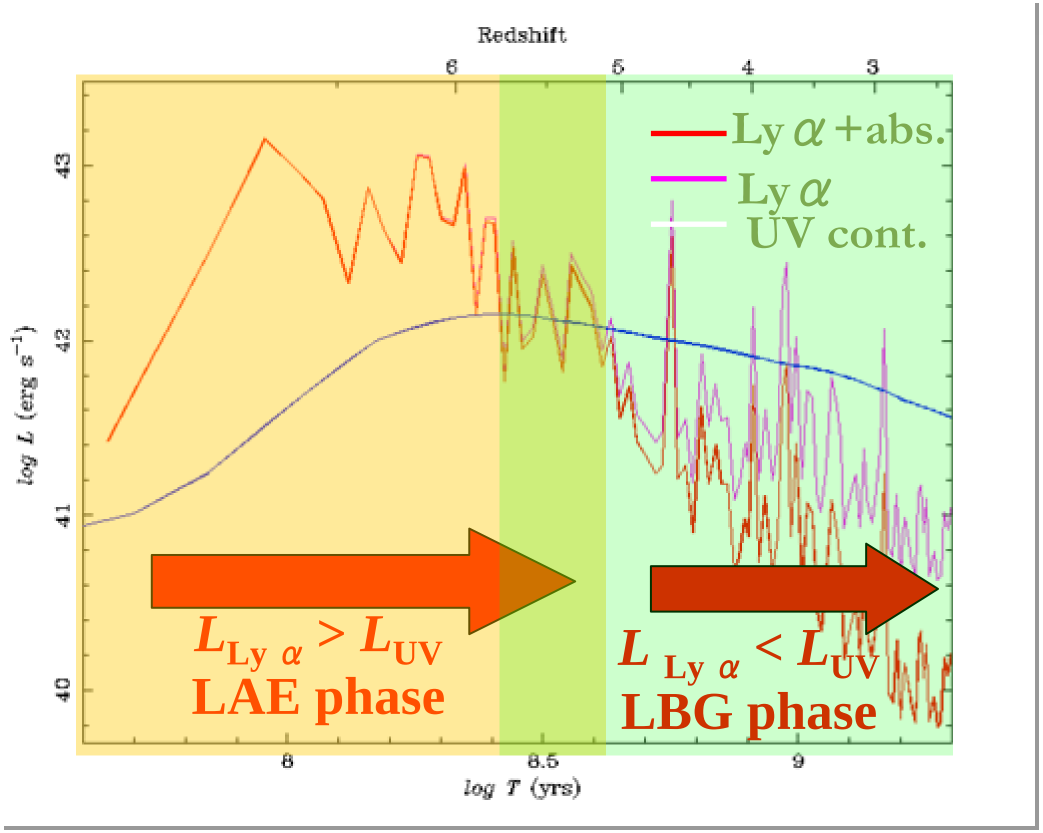

The results of our simulation indicate the possible link among LAEs and LBGs.
The simulated post-starburst galaxy with the age of 1 Gyr can correspond to LBGs.
It is implied that LBGs are the subsequent phase of LAEs.

- 宇宙論的シミュレーション

- 物理的シミュレーション
  - マイナーマージャーモデル
    Mori & Umemura (2006)
  - シングルコラプスモデル
    Fixed potential of Dark matter halo
    Constant gas density
    Rigid rotation　$\lambda = 0.05$

Model and parameters

- Total mass : $10^{8\text{-}12}\ M_{\odot}$, Total gas mass: $1.3\text{x}10^{7\text{-}11}\ M_{\odot}$

  Ω_M=0.3, Ω_Λ=0.7, h=0.7, z=7.8, Ω_b=0.024 h^{-2}
- Dark Matter: Navarro-Frenk-White density
- Gas: Constant density
- Star formation :

  $\tau_{cool} < \tau_{ff} < \tau_{cros}$

  ρ crit=0.1 cm^{-3}

  $d\rho_* / dt = \rho_g / \tau_{ff}$

  Salpeter's IMF
- Supernova feedback:

  E_{SN} = 10^{51} erg / SN

  Oxygen : 2.4 $M_{\odot}$ / S

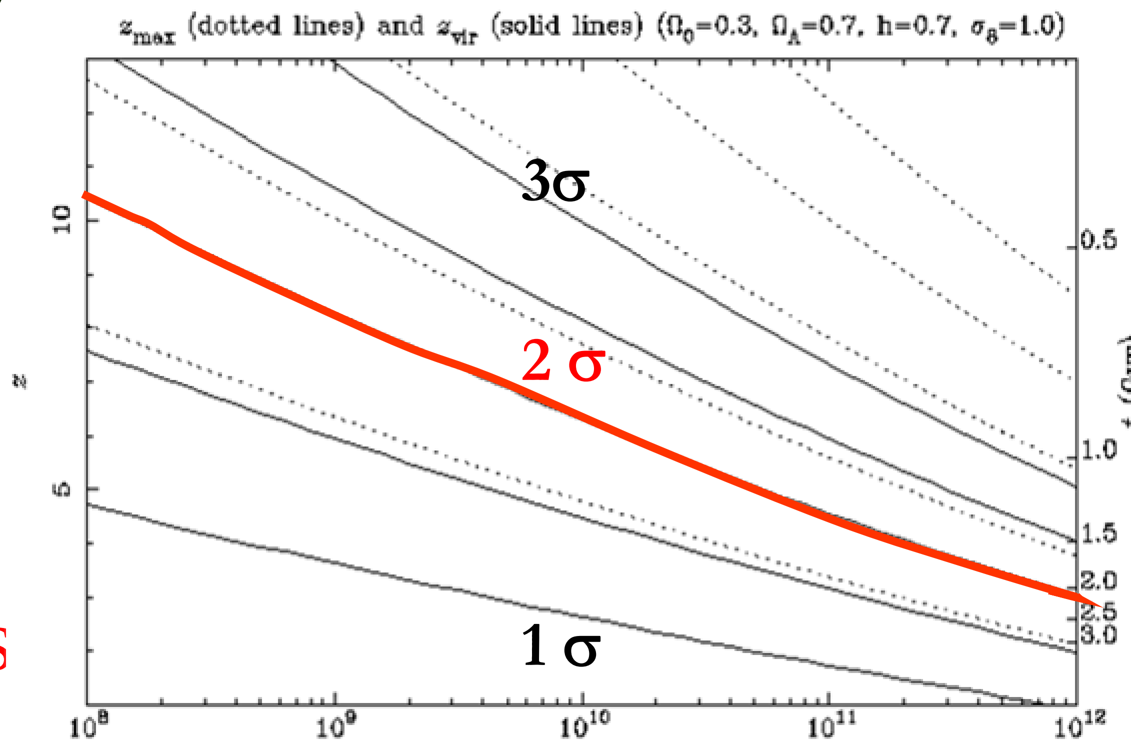

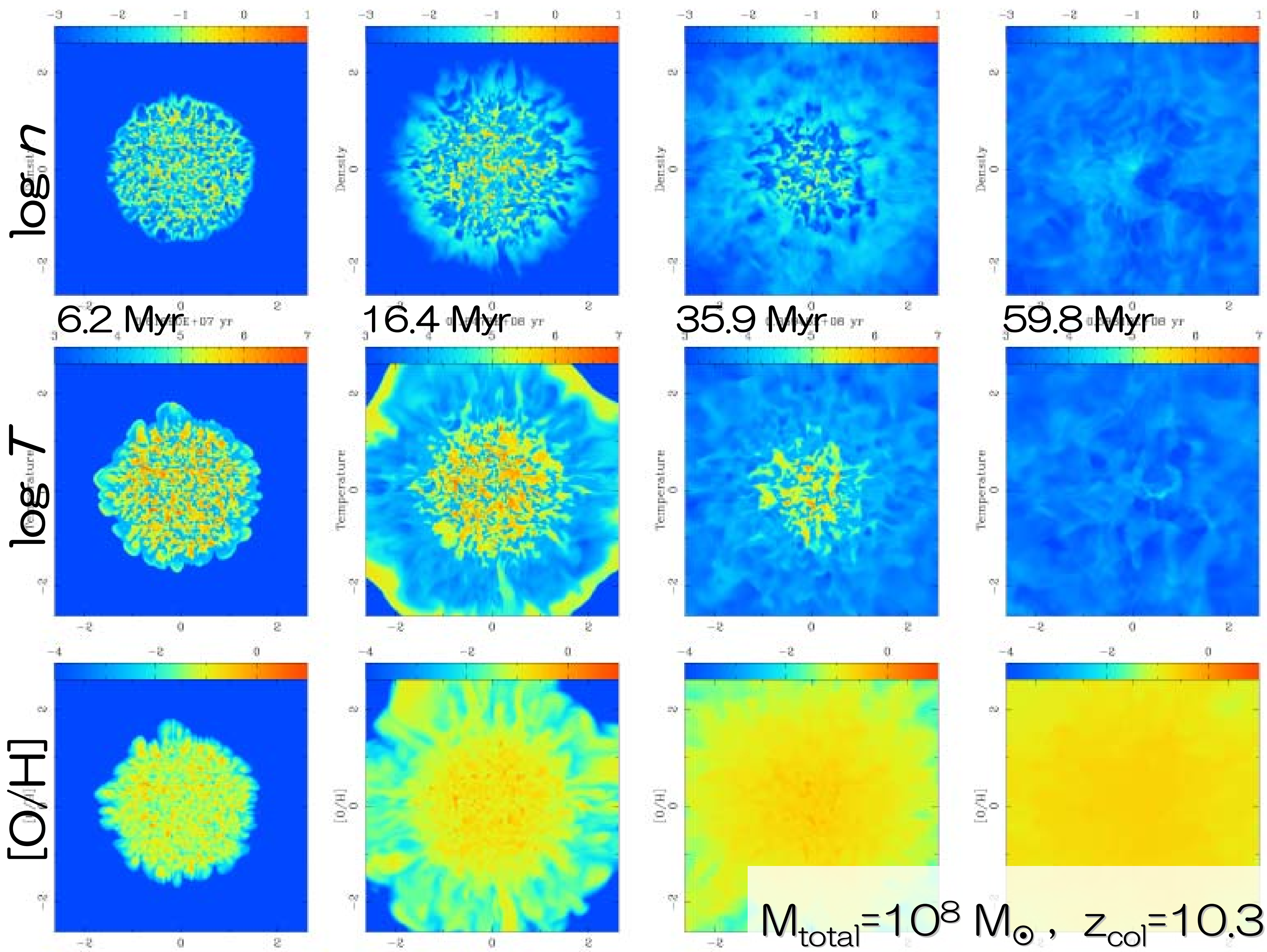

log n
log T
[O/H]
6.2 Myr
16.4 Myr
35.9 Myr
59.8 Myr
Density
Temperature
[O/H]
$M_{total}=10^8\ M_\odot$, $z_{col}=10.3$

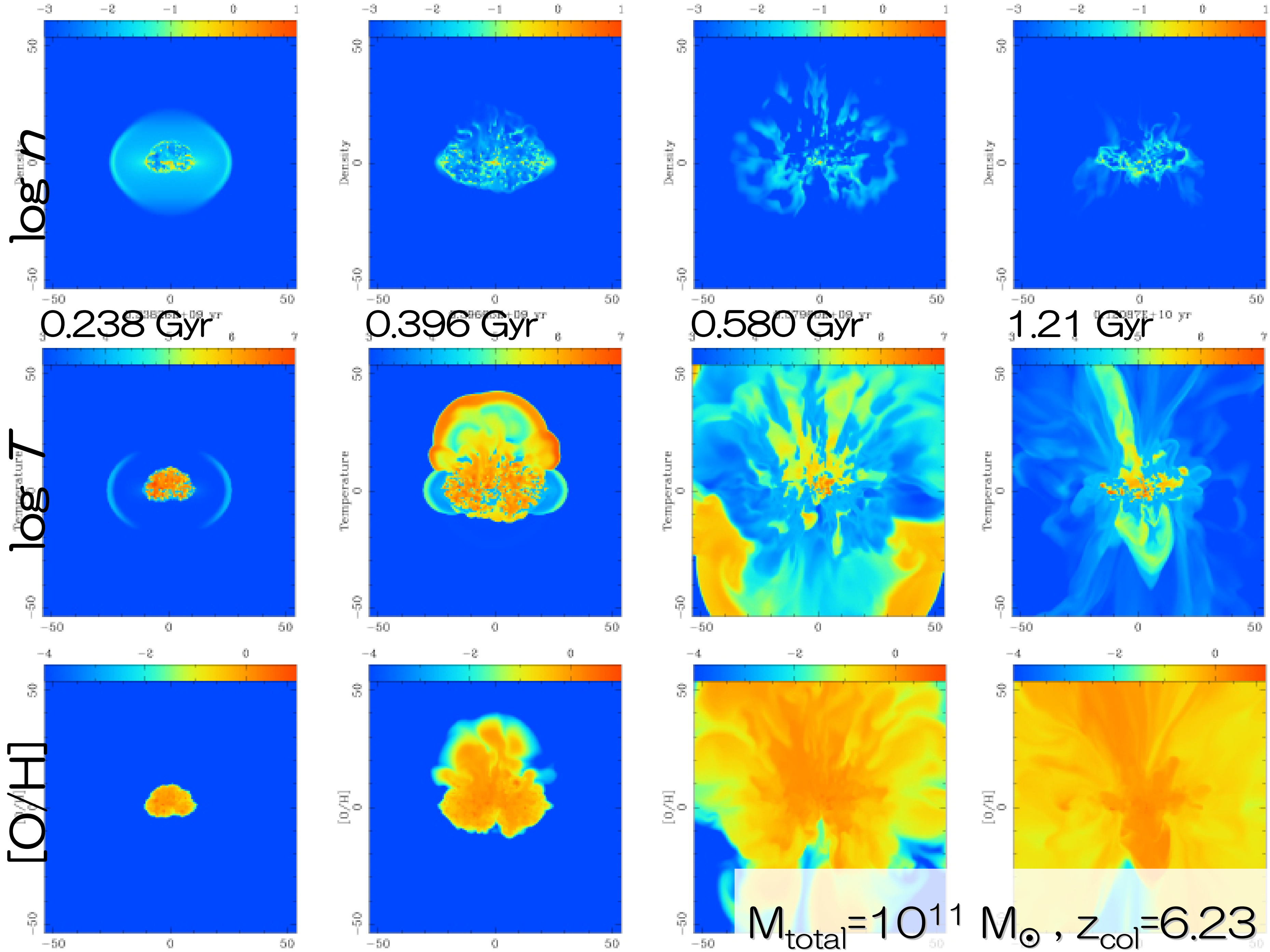
log n
log T
[O/H]
0.238 Gyr
0.396 Gyr
0.580 Gyr
1.21 Gyr
M_total=10^11 M_⊙ , z_col=6.23

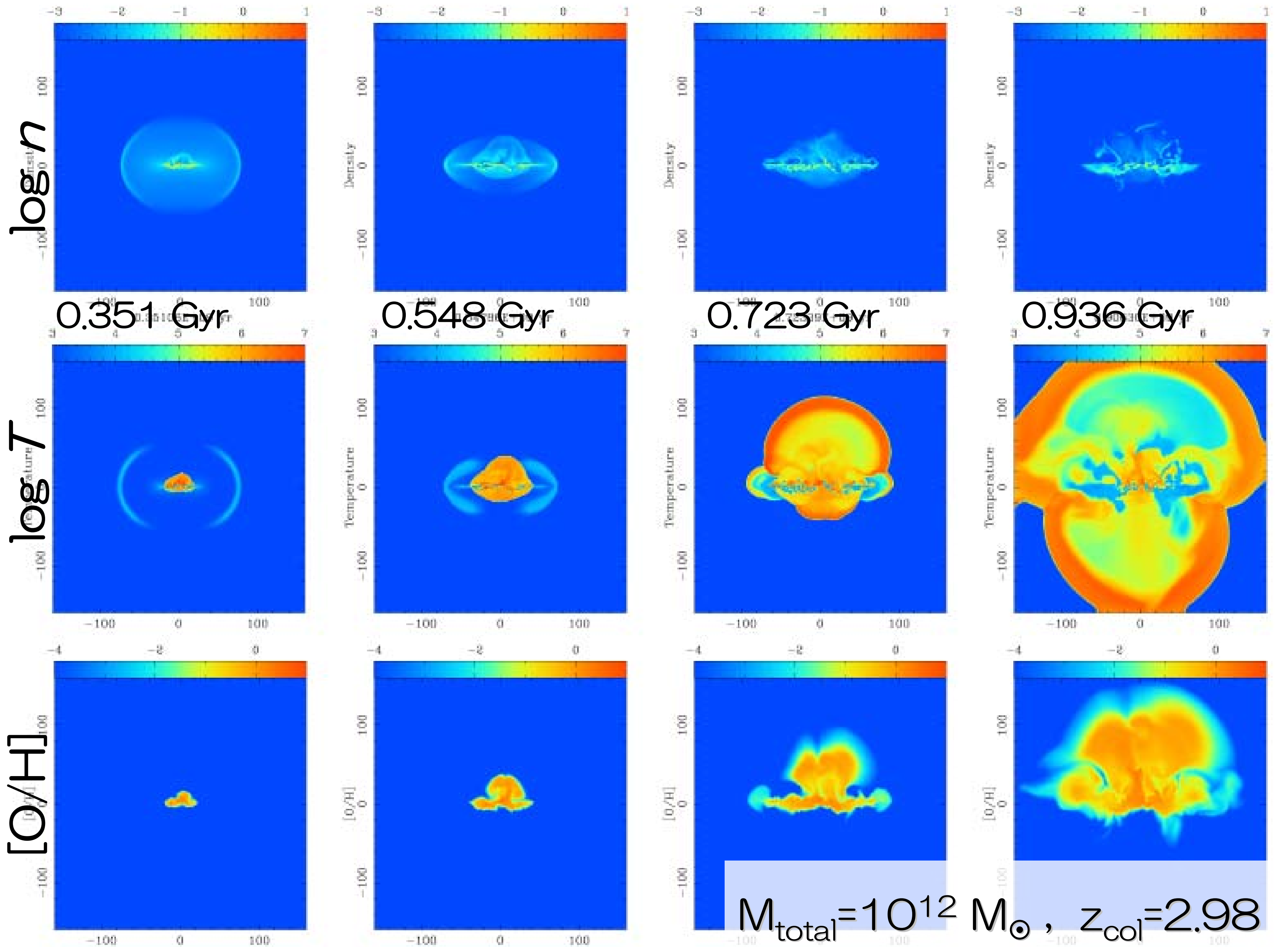

log n
log T
[O/H]
0.351 Gyr
0.548 Gyr
0.723 Gyr
0.936 Gyr
Density
Temperature
[O/H]
$M_{total}=10^{12}\ M_{\odot}$, $z_{col}=2.98$

Evolution of stellar component

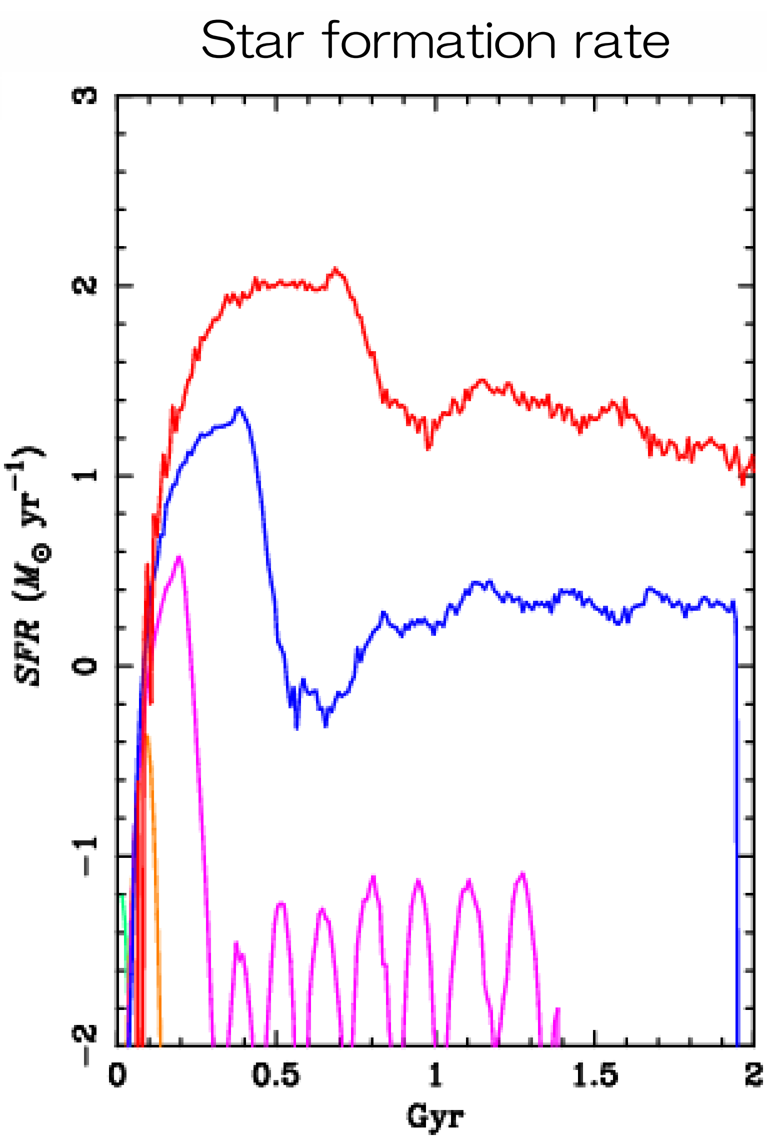

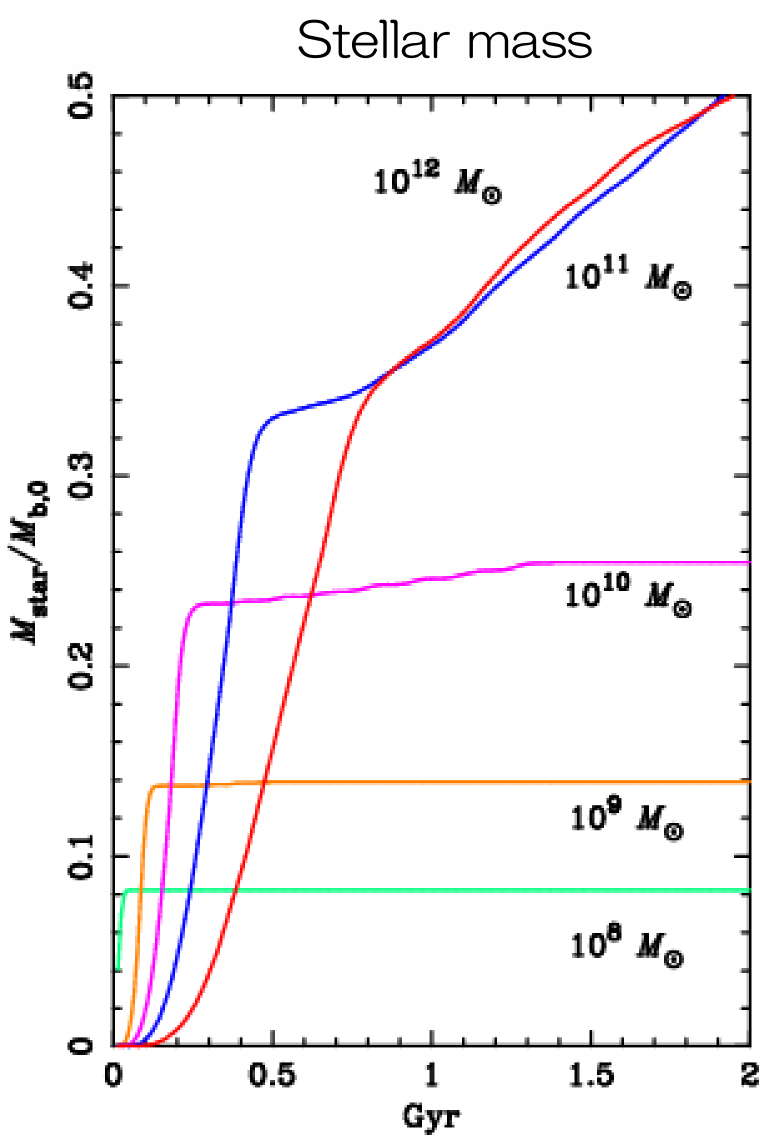

Evolution of gas component

Gas mass

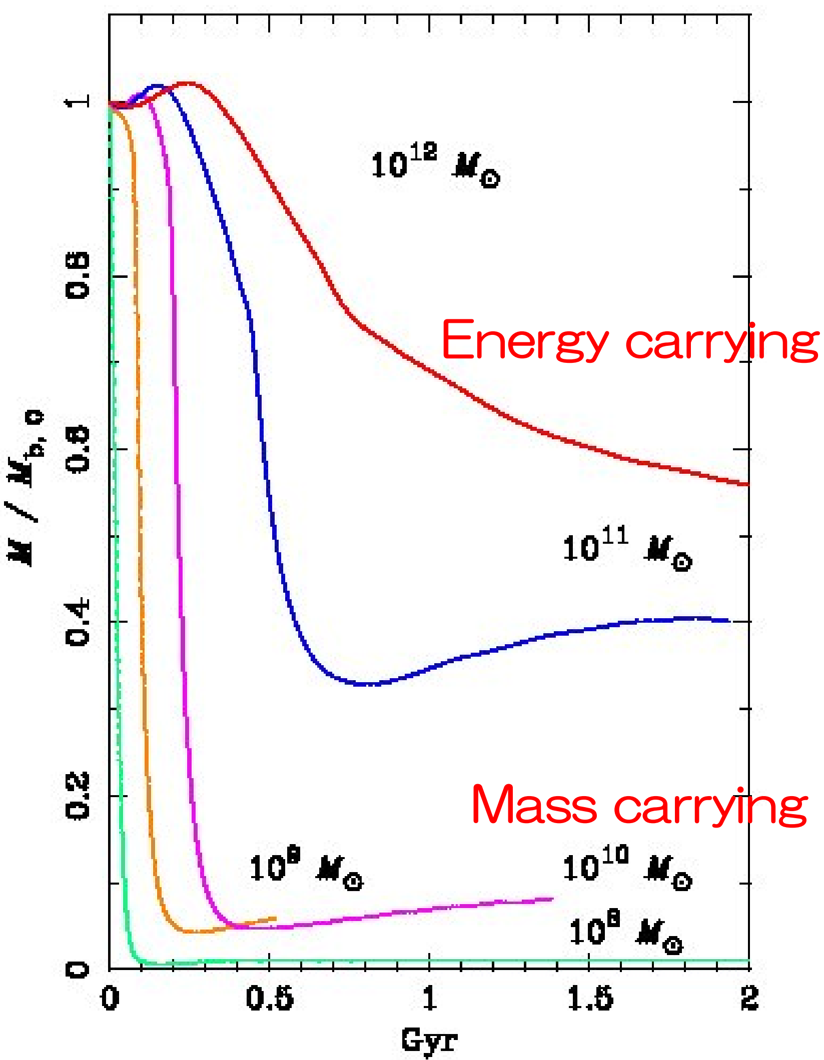

Mean metallicity

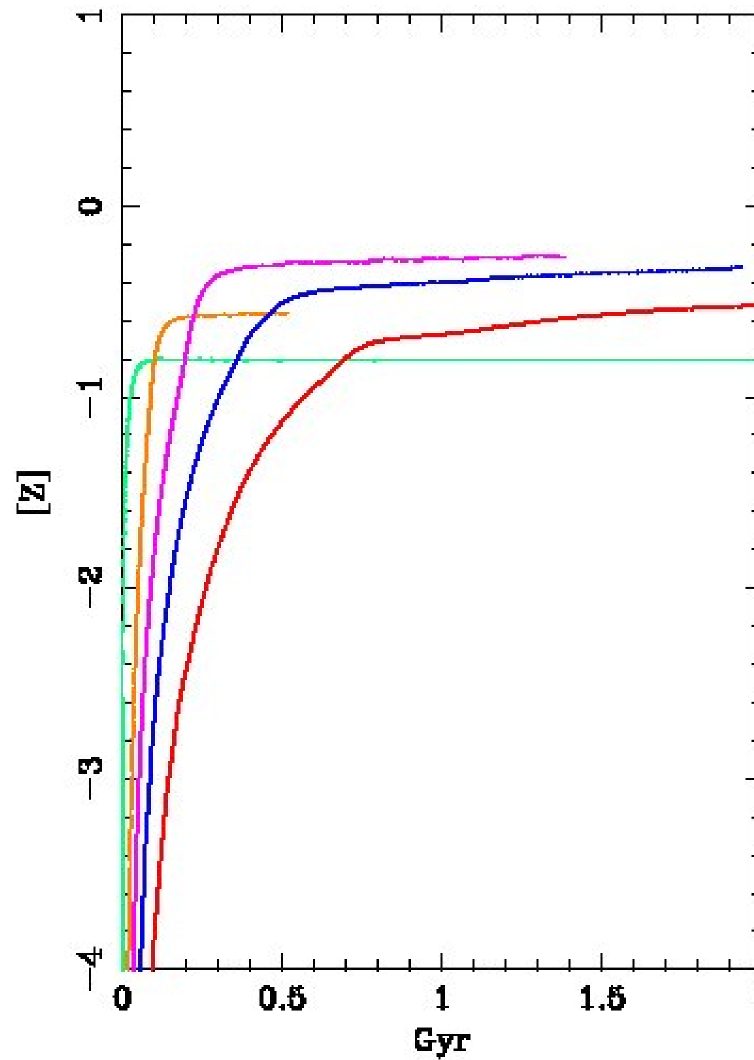

Filling factor

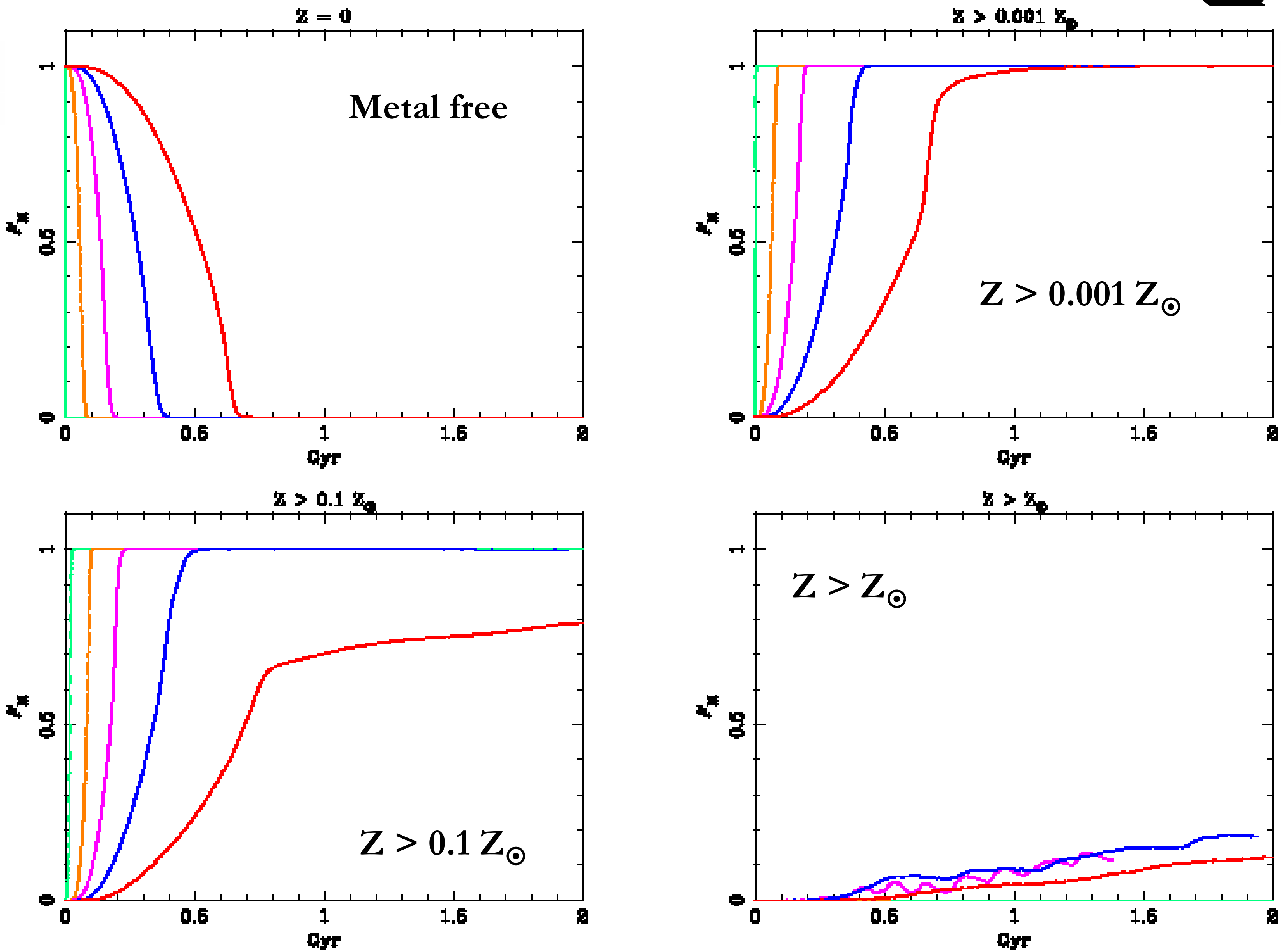

Lyman alpha emission

Gas cooling radiation

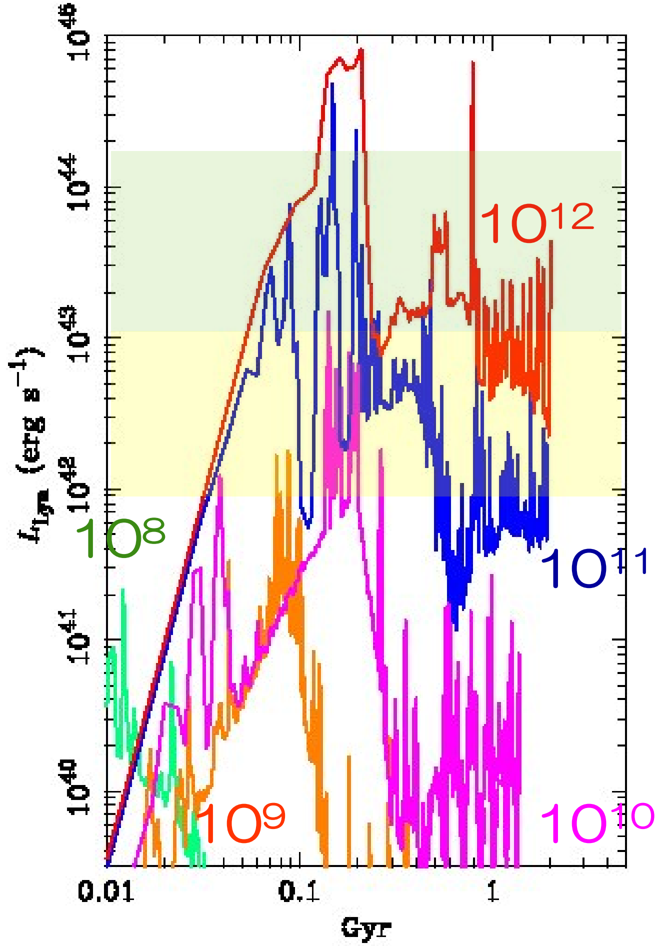

Stellar origin (HII)

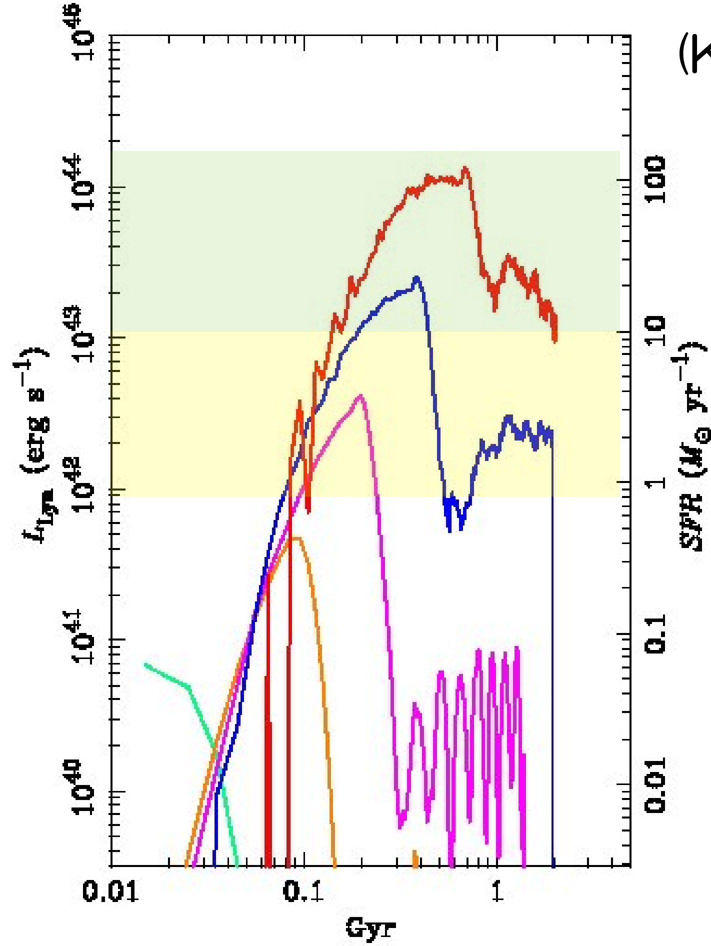

SFR
$= 9.1 \times 10^{-43} L_{ly\alpha}$
(Kennicutt 1998)

Origin of Lyman alpha photon

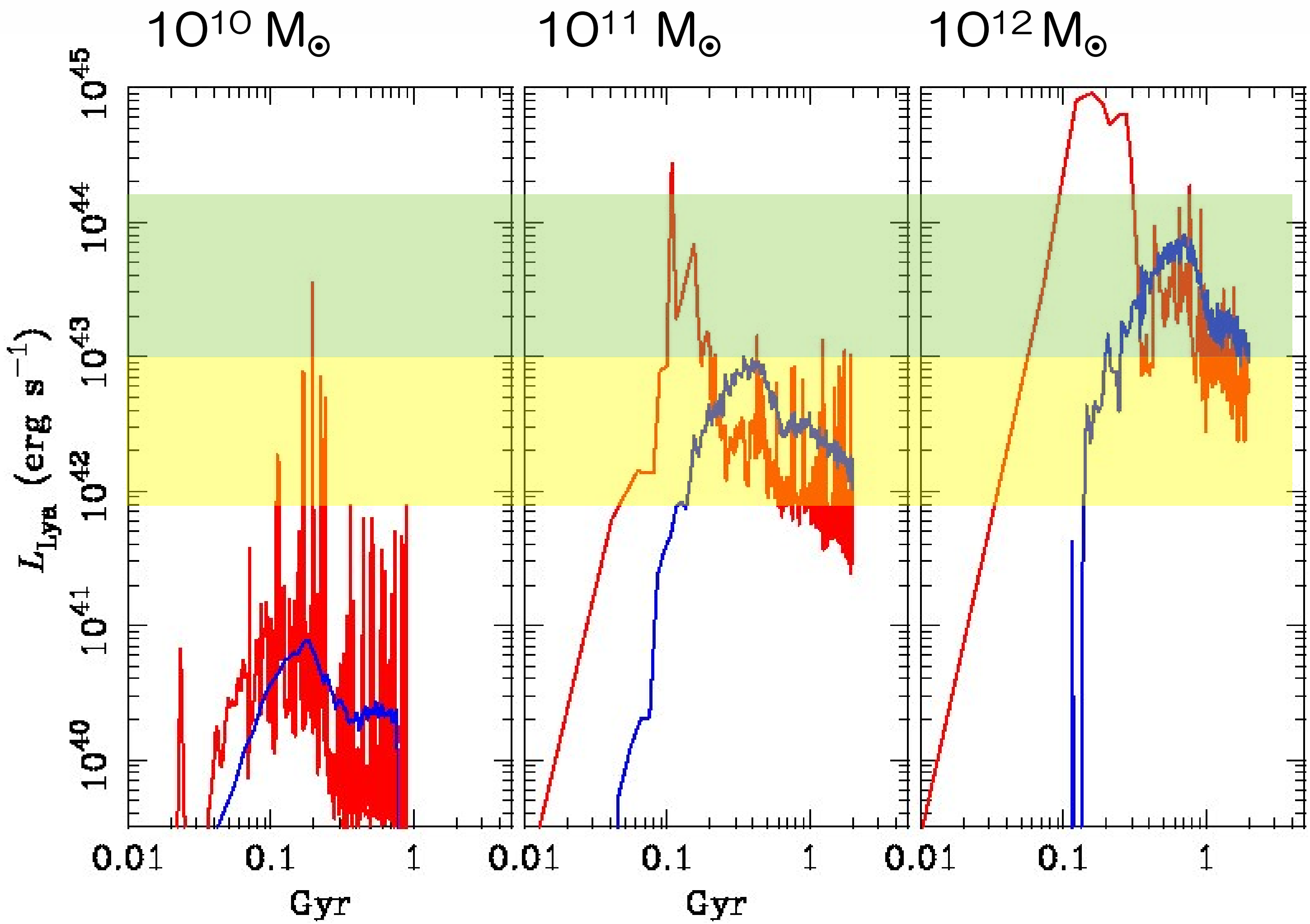

Red: cooling, blue: stellar

Summary

- We simulated a forming galaxy using a high resolution hydrodynamic simulation, where supernova remnants are resolved with sufficient accuracy.
- We have suggested that Lyman α emitters can be identified with primordial galaxies catched in a supernova-dominated phase.
- The bubbly structures produced by multiple supernova explosions are quite similar to the observed features in Lyman α surface brightness of Lyman α blobs.
- The resultant Ly α luminosity can account for the observed luminosity of Lyman α emitters.
- After 1 billion years the simulated galaxy is dominated by stellar continuum radiation and looks like the Lyman break galaxies. At this stage, the metal abundance reaches already the level of solar abundance.